

Can monodisperse microbubble-based three-dimensional contrast-enhanced ultrasound reduce quantitative heterogeneity? An in vitro study

*Qiao Zheng^{1,A–F}, *Si-Min Ruan^{2,A–F}, Chun-Yang Zhang^{2,B,C}, Zhong Cao^{3,B,C}, Ze-Rong Huang^{2,E}, Huan-Ling Guo^{2,B,C}, Xiao-Yan Xie^{2,E,F}, Ming-De Lu^{2,4,E,F}, **Wei Wang^{2,A,E,F}, **Li-Da Chen^{2,A,E,F}

¹ Department of Medical Ultrasonics, Fetal Medical Center, The First Affiliated Hospital of Sun Yat-sen University, Guangzhou, China

² Department of Medical Ultrasonics, Ultrasonics Artificial Intelligence X-Lab, Institute of Diagnostic and Interventional Ultrasound, The First Affiliated Hospital of Sun Yat-sen University, Guangzhou, China

³ Department of Biomedical Engineering, School of Engineering, Sun Yat-sen University, Guangzhou, China

⁴ Department of Hepatobiliary Surgery, The First Affiliated Hospital of Sun Yat-sen University, Guangzhou, China

A – research concept and design; B – collection and/or assembly of data; C – data analysis and interpretation;

D – writing the article; E – critical revision of the article; F – final approval of the article

Advances in Clinical and Experimental Medicine, ISSN 1899–5276 (print), ISSN 2451–2680 (online)

Adv Clin Exp Med. 2022;31(3):307–315

Address for correspondence

Li-Da Chen

E-mail: chenlda@mail.sysu.edu.cn

Funding sources

Natural Science Foundation of China (Grant No. 81971630); Science and Technology Program of Guangzhou, China (Grant No. 201904010187); Kelin New Star Program for Talents of The First Affiliated Hospital of Sun Yat-sen University, Guangzhou, China (Grant No. Y50168).

Conflict of interest

None declared

* Qiao Zheng and Si-Min Ruan contributed equally to this work.

** Wei Wang and Li-Da Chen were co-corresponding authors to this work.

Received on June 11, 2021

Reviewed on October 28, 2021

Accepted on November 4, 2021

Published online on December 2, 2021

Cite as

Zheng Q, Ruan SM, Zhang CY, et al. Can monodisperse microbubble-based three-dimensional contrast-enhanced ultrasound reduce quantitative heterogeneity?

An in vitro study. *Adv Clin Exp Med.* 2022;31(3):307–315.

doi:10.17219/acem/143585

DOI

10.17219/acem/143585

Copyright

Copyright by Author(s)

This is an article distributed under the terms of the Creative Commons Attribution 3.0 Unported (CC BY 3.0) (<https://creativecommons.org/licenses/by/3.0/>)

Abstract

Background. Heterogeneity within the tumor may cause large heterogeneity in quantitative perfusion parameters. Three-dimensional contrast-enhanced ultrasound (3D-CEUS) can show the spatial relationship of vascular structure after post-acquisition reconstruction and monodisperse bubbles can resonate the ultrasound pulse, resulting in the increase in sensitivity of CEUS imaging.

Objectives. To evaluate whether the combination of 3D-CEUS and monodisperse microbubbles could reduce the heterogeneity of quantitative CEUS.

Materials and methods. Three in vitro perfusion models with perfusion volume ratio of 1:2:4 were set up. Both quantitative 2D-CEUS and 3D-CEUS were used to acquire peak intensity (PI) with 2 kinds of ultrasound agents. One was a new kind of monodisperse bubbles produced in this study, named Octafluoropropane-loaded cerasomal microbubbles (OC-MBs), the other was SonoVue®. The coefficient of variation (CV) was calculated to evaluate the cross-sectional variability. Pearson's correlation analysis was used to assess the correlation between weighted PIs (average of PIs of 3 different planes) and perfusion ratios.

Results. The average CVs of quantitative 3D-CEUS was slightly lower than that of 2D-CEUS (0.41 ± 0.17 compared to 0.55 ± 0.26 , $p = 0.3592$). As for quantitative 3D-CEUS, the PI of the OC-MBs has shown better stability than that of SonoVue®, but without a significant difference (average CVs: 0.32 ± 0.19 compared to 0.50 ± 0.10 , $p = 0.0711$). In the 2D-CEUS condition, the average CVs of OC-MBs group and SonoVue® group were 0.68 ± 0.15 and 0.41 ± 0.17 ($p = 0.2747$). As for 3D-CEUS condition, using OC-MBs group and SonoVue®, the r-values of the weighted PI and perfusion ratio were 0.8685 and 0.5643, respectively, while that of 2D-CEUS condition were 0.7760 and 0.3513, respectively.

Conclusions. Our in vitro experiments showed that OC-MBs have the potential in acquiring more stable quantitative CEUS value, as compared to the SonoVue® in 3D-CEUS condition. The combination of 3D-CEUS and OC-MBs can reflect perfusion volume more precisely and may be a potential way to reduce quantitative heterogeneity.

Key words: ultrasonography, three-dimensional imaging, in vitro technique, contrast agent

Introduction

Contrast-enhanced ultrasound (CEUS) is a noninvasive imaging method, using ultrasound contrast agent (UCA) and low mechanical index (MI) ultrasound for dynamic blood perfusion observation in the target tissue. It has been applied in the detection and differential diagnosis of solid tumors, the assessment of nonsurgical treatment and the evaluation of left ventricular function. As is commonly known, one of the inherent limitations of CEUS is its subjectivity. In contrast with traditional CEUS, quantitative CEUS with dedicated software can detect lesions with abnormal perfusion more sensitively.¹ A multitude of quantitative parameters can be used as imaging biomarkers. They can improve the diagnostic efficacy as well as the detection rate of atypical lesions.^{2–4}

However, the quantitative CEUS faces 2 major dilemmas. First, the widely used quantitative two-dimensional CEUS (2D-CEUS) could only obtain a single plane of tumor perfusion.⁵ Due to tumor necrosis, hemorrhage and hypoxia, there is a large heterogeneity within the tumor, which leads to the complexity of blood supply of tumor. Quantitative 2D-CEUS could not fully demonstrate the spatial features of the tumor internal environment,⁶ which would result in greater heterogeneity of quantitative parameters in different planes.⁷ Second, commercially available UCA typically consists of a suspension of phospholipid-coated microbubbles with radius ranging from 1 μm to 10 μm in diameter.⁸ Upon exposure to ultrasound, the microbubbles oscillate and generate harmonic echoes, which make the visualization and quantification of organ perfusion possible. The strength of harmonic signal is proportional to the 6th power of the radius of UCA microbubble,⁹ which means that polydisperse microbubbles can also affect the quantitative results in CEUS. The monodisperse microbubble suspension is narrowband and has acoustically uniform response.¹⁰ Therefore, by using monodisperse bubbles resonating with ultrasound pulse, the sensitivity of CEUS imaging can be increased by 2 to 3 orders of magnitude.¹¹

Herein, we need to reduce the tumor quantitative heterogeneity taking into account 2 aspects. First, the three-dimensional CEUS (3D-CEUS) will be used to reconstruct the entire target lesion stereoscopically combining x, y and z axes through software and improve the accuracy of tumor angiogenesis quantification.¹² One of our previous in vitro studies has found that quantitative 3D-CEUS is more representative of the perfusion volume and with lower heterogeneity when compared with 2D-CEUS.⁷ Second, a new kind of monodisperse microbubbles (Octafluoropropane-loaded cerasomal microbubbles (OC-MBs))¹³ with uniform size and long sonographic duration will be used to resonate with ultrasound pulse.

Objectives

In this study, an in vitro model was designed to observe whether the combination of 3D-CEUS and monodisperse microbubbles can reduce the heterogeneity of quantitative CEUS.

Materials and methods

Materials

Hexadecylamine was obtained from Tokyo Pharmaron Industrial Co. (Tokyo, Japan). Bromohexadecane was obtained from Shanghai Aladdin Co. (Shanghai, China). Poly (sodium 4-styrenesulfonate) (PSS; ~70,000 MW), poly (allylamine hydrochloride) (PAH; ~15,000 MW) and methyl thiazolyl tetrazolium (MTT) were synthesized by Sigma–Aldrich (St. Louis, USA). Sodium carbonate (Na_2CO_3), calcium nitrate tetrahydrate ($\text{Ca}(\text{NO}_3)_2 \cdot 4\text{H}_2\text{O}$) and disodium ethylenediaminetetraacetate dihydrate (EDTA) were obtained from Guangzhou Chemical Reagent Factory (Guangzhou, China).

Fetal calf serum, tryptase, Dulbecco's modified Eagle's medium (DMEM) and Penicillin-Streptomycin were purchased from Thermo Fisher Scientific (Waltham, USA). Human umbilical vein endothelial cells (HUVEC) and HepG2 cells were purchased from Sun Yat-sen Animal Experimental Center (Guangzhou, China).

Synthesis of Si-lipid

The method of N-[N-(3-triethoxysilyl) propylsuccinamoyl] dihexadecylamine (Si-lipid) synthesis was reported previously.¹⁴

Preparation of CaCO_3 (PSS-PAH) microspheres

The PSS-doped CaCO_3 microspheres with uniform diameter were synthesized using colloidal aggregation of Na_2CO_3 and $\text{Ca}(\text{NO}_3)_2$.^{15,16} First, 590 mL of $\text{Ca}(\text{NO}_3)_2 \cdot 4\text{H}_2\text{O}$ (0.025 M) and 400 mg of PSS were combined as an aqueous solution, into which 265 mL of Na_2CO_3 (0.025 M) solution was rapidly added under magnetic agitation (600 rpm) for 15 s. Then, the solution was kept for 10 min at 15°C. The PSS-doped CaCO_3 microspheres were acquired and washed by centrifugation with deionized water (4000 rpm, 10 min). The adsorption of PAH onto the PSS-doped CaCO_3 microspheres was conducted in a 0.1 M NaCl solution with 80 mg of PAH. After 15 min, free-PAH was removed and the microbubbles were washed twice with deionized water. Then, CaCO_3 (PSS-PAH) microspheres were obtained.

Preparation of octafluoropropane(OFP)-loaded cerasomal microbubbles (OC-MBs)

The method of synthesis has been previously described.¹⁷ Under water bath sonication, 10 mg of Si-lipid dissolved in 200 μ L of ethanol (pH = 3) was injected into 5 mL of CaCO₃(PSS-PAH) (4 mg/mL) microsphere aqueous solution in a vial. After injection, the vial was kept in water bath sonication for 2 min. Then, the suspensions were incubated at room temperature for 12 h to form a siloxane network on the surface of the microspheres. The free Si-lipid was removed with centrifugation. The EDTA 2Na solution (0.2M) was utilized to remove the CaCO₃ core of the microspheres 3 times. The obtained microbubbles were freeze-dried with mannitol (10% w/w). Finally, the bottle was filled with OFP to acquire OC-MBs.

Characterization of OC-MBs

The morphology of 2 kinds of microbubbles (OC-MBs and SonoVue[®]) was observed using optical microscopy (CKX41; Olympus Corp., Tokyo, Japan). The OC-MBs were also observed with field emission scanning electron microscopy (FE-SEM, Zeiss-Ultra 55; Zeiss Co., Oberkochen, Germany). Twenty microliters of OC-MBs suspension was casted onto copper foil. Then, the specimens were sputtered with gold for 5–10 min and inspected using a FE-SEM with 10 kV accelerating voltage.

Hemolysis assay

The hemolysis assay was conducted according to the previous studies.^{18,19} Human red blood cells were separated from the whole blood through centrifugation for 10 min at 1500 rpm and purified with sterile isotonic phosphate-buffered saline (PBS) via 6 successive washes. The packed red blood cells were suspended in PBS buffer diluting to a concentration of 4.0×10^8 /mL. Then, 0.5 mL of the diluted human red blood cell suspension was added to 1.5 mL of deionized water (positive control), sterile isotonic PBS (negative control) or PBS buffer containing OC-MBs with concentration of 50 μ g/mL, 100 μ g/mL, 200 μ g/mL, 400 μ g/mL, and 800 μ g/mL, respectively. After gentle shaking, the samples were allowed to stand at 37°C for 2 h. Finally, after centrifugation for 10 min at 1500 rpm, the supernatants were measured at 541 nm using UV-DU730 absorption spectrophotometer (Beckman Coulter, Inc., Brea, USA) to analyze the release of hemoglobin. The hemolysis percentage of each group was calculated according to the following formula (Eq. 1)^{20,21}:

$$\text{percent hemolysis (\%)} = \frac{A_{\text{sample}} - A_{\text{negative}}}{A_{\text{positive}} - A_{\text{negative}}} \times 100 (\%) \quad (1)$$

where A_{sample} was the absorbance of the supernatant of the sample; A_{positive} was the absorbance of the supernatant of positive group (deionized water); and A_{negative} was the absorbance of the supernatant of negative group (PBS buffer).

Cytotoxicity of OC-MBs

The cytotoxicity of OC-MBs was evaluated using the standard MTT assay.²² The HUVECs and the HepG2 cells were seeded in each of two 96-well plates and cultured in DMEM with 10% fetal calf serum (v/v) overnight. Then, the cells were incubated for 24 h and 48 h in the presence of OC-MBs concentrations of 25 μ g/mL, 50 μ g/mL, 100 μ g/mL, 200 μ g/mL, 400 μ g/mL, and 800 μ g/mL, respectively. Fresh DMEM was added to the negative control group. Then, the culture medium was taken out and the cells were washed with PBS. Fresh medium (100 μ L) and 20 μ L of MTT assay (5.0 mg/mL) per well were added to all wells and the wells were incubated for 4 h. After removing the medium, the resultant formazan salt crystals were dissolved in 150 μ L of dimethyl sulfoxide (DMSO) and analyzed on a microplate reader (Synergy 4; BioTek, Winooski, USA) at 570 nm. A pure DMSO empty group was also analyzed. The percent of cell survival rate was calculated using the following formula (Eq. 2):

$$\text{cell survival rate (\%)} = \frac{A_{\text{sample}} - A_{\text{empty}}}{A_{\text{positive}} - A_{\text{empty}}} \times 100 (\%) \quad (2)$$

where A_{sample} was the absorbance of supernatant of sample; A_{negative} was the absorbance of supernatant of negative group (fresh DMEM) and A_{empty} was the absorbance of supernatant of empty group (pure DMSO).

In vitro experiment of OC-MBs

Establishment of the in vitro model

Three polyvinyl chloride pipes with outer diameter of 2 mm and an inner diameter of 1 mm were divided into 3 parts (inflow part, perfusion model part and outflow part) with tin foil. The perfusion model was located in the middle of the tubes with a length of the pipe of 8 cm, 16 cm and 32 cm, respectively, to simulate the different blood supply levels of the tumor. The perfusion model was divided into annular (8 cm) and spherical (16 cm and 32 cm) model. The pipe could not be folded and the inner diameter was not to be too narrow. The volume ratio of the perfusion model was 1:2:4.

The perfusion model was fixed in a water tank with sound-absorbing sponges on the base of the tank (Fig. 1). The 3D ultrasonic probe was fixed upon the perfusion model below the water surface. The inflow end was connected to the syringe pump (WZ-50C6; Smiths Medical, Minneapolis, USA) to ensure that the contrast medium was perfused at a constant rate (200.0 mL/h). The outflow end was put into a 1000 mL beaker.

Image acquisition and quantitative analysis of CEUS

Contrast-enhanced ultrasound (CEUS) examinations were performed using an Aplio 500 ultrasound scanner (Toshiba Medical Systems, Tokyo, Japan) with a 3D imaging

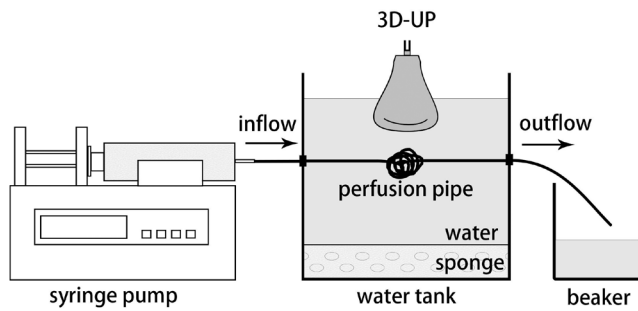


Fig. 1. Device schematic diagram of in vitro experiment

UP – ultrasonic probe.

probe (PVT375MV, frequency: 2–8 MHz; Toshiba Medical Systems). The probe was fixed with a shelf under the water surface and above the perfusion model. The maximum cross section of the perfusion model was regarded as the 0° plane. Then, the probe was rotated to obtain 45° plane and 90° plane images.

Two-dimensional ultrasound (2D-US), real-time 2D-CEUS and 3D-CEUS were performed in each plane. Two kinds of ultrasound contrast agents, including OC-MBs and SonoVue® (Bracco Imaging, Milan, Italy), were dissolved in 0.9% saline with microbubble concentration of $4 \times 10^6/\text{mL}$ and gently shaken until they became a milky white suspension. The UCA was injected through the inner tube at a constant speed of 200 mL/h. The duration of each imaging was 2 min and it was repeated 6 times. During the interval of each measurement, 0.9% saline was used to rinse the tubes in order to remove the microbubbles attaching on the tube wall, which might affect the experimental results. The original image data were stored for quantitative analysis.

The online software analysis package used was Aplio 500 v. 3.7 (CHI-Q) (Toshiba Medical Systems). This study focused on the peak intensity (PI), the maximum average peak intensity of flow perfusion in the region of interest (ROI). It has been reported that PI can accurately reflect

the blood volume of the tissue when the instrument settings and the UCA dose remain unchanged.²³

Statistical analysis

Continuous data following normal distribution were expressed as the mean \pm standard deviation (SD). The paired sample t-test was applied to evaluate the differences of the average of coefficient of variation (CV). Pearson's correlation analysis was used to determine the correlation between weighted PI (the average value of PI at 0°, 45° and 90° planes) and the 2 imaging methods, as well as the correlation between weighted PI and perfusion volume (1:2:4). The level of significance was set at a two-tailed $p < 0.05$. The statistical analysis was performed using IBM SPSS v. 22.0 software (IBM Corp., Armonk, USA).

Results

Homogeneity of OC-MBs

The image of the optical microscopy and the transmission electron microscopy (TEM) of OC-MBs were shown in Fig. 2A and Fig. 2B. The average diameter of OC-MBs was 2.0 μm , with high size uniformity. The image of the optical microscopy of SonoVue® suspension and OC-MBs were compared in Fig. 3A and Fig. 3B. The OC-MBs microbubbles had higher homogeneity.

Hemolysis assay and in vitro cytotoxicity of OC-MBs

The blood biocompatibility of OC-MBs should be considered for using as an UCA. Hemolysis assay was conducted to evaluate the blood compatibility. When hemolysis occurs, the hemoglobin presented in red blood cells will be released into solution, coloring it red. The density

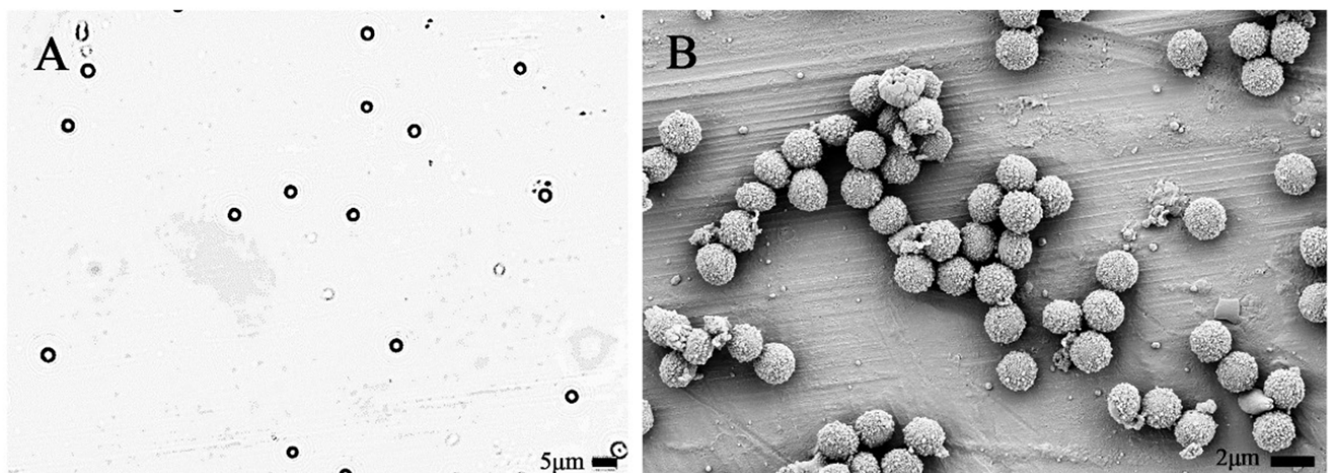


Fig. 2. Optical microscope image ($\times 400$) (A) and scanning electron microscopy image (B) of octafluoropropane-loaded cerasomal microbubbles (OC-MBs) of 2.0 μm

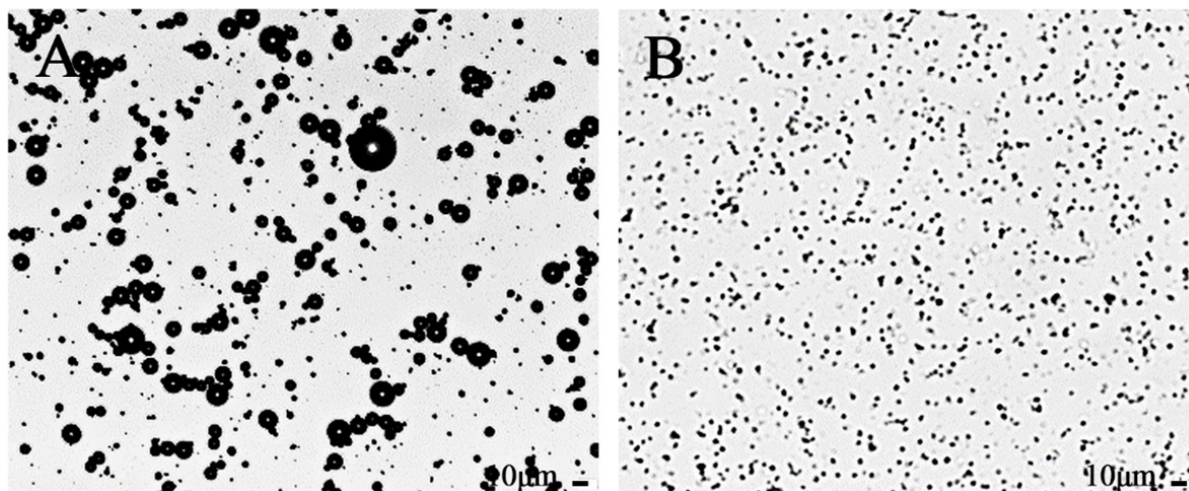


Fig. 3. Optical microscope image (x200) of SonoVue® (A) and octafluoropropane-loaded cerasomal microbubbles (OC-MBs) (B)

of this red color is correlated with hemolytic activity and can be estimated by measuring the ultraviolet (UV) absorbance of a supernatant at 541 nm. The tube with the highest concentration of OC-MBs (800 μg/mL) was light red (Fig. 4). The solution of concentration ranged from 50 μg/mL to 400 μg/mL and was nearly transparent. The OC-MBs only experienced approx. 1.3% hemolysis at the highest experimental concentration of 800 μg/mL (Fig. 4). Consequently, it can be concluded that OC-MBs have negligible hemolytic activity.

The cytotoxicity of an UCA is vital to its biomedical application. In vitro cytotoxicity was tested on HUVEC and HepG2 cell lines. An MTT assay was used to estimate the cytotoxicity of OC-MBs. As shown in Fig. 5, HUVECs retained 88% cell viability after incubation with

OC-MBs for 48 h at a high concentration of 800 μg/mL, while the cell viability of HepG2 cell was higher than 95%. The cell viability presented no significant difference when measurements at 24 h and 48 h were compared.

The OC-MBs present prominent biocompatibility and may have the potential to use them as a new UCAs in vivo.

Ultrasound images of 2 UCAs

The model had an irregular shape on the imaging plane, and the diameter of the tube was uniform in structure. The ultrasound images of 2 UCAs were shown in Fig. 6 (OC-MBs: A and B, SonoVue®: C and D). When 2D-CEUS was used, the signals were similar for both UCAs (Fig. 6A,C). Yet, for 3D-CEUS, OC-MBs group could obtain clearer signals as compared to SonoVue® group, and the boundary of the perfusion pipe was sharper in the OC-MBs group (Fig. 6B,D).

Variability of quantitative CEUS of 2 UCAs in 3 different sections

The PI values of different perfusion models, UCAs and CEUS mode are shown in Table 1 and Table 2. The PI of each model in different cross sections was the average of 6 measurements and was shown as the mean ±SD. Each CV was calculated with the SD and the mean of the PI of 3 different cross sections in the same perfusion model, CEUS mode and UCA. The average CV of 3D-CEUS was slightly lower than that of 2D-CEUS, without significant difference (0.41 ±0.17 compared to 0.55 ±0.26, p = 0.3592, T = -1.009, degrees of freedom (df) = 5) (Table 3). When we used the 3D-CEUS, the average CVs of OC-MBs group and SonoVue® group were 0.32 ±0.19 and 0.50 ±0.10, respectively. The PI of the OC-MBs has shown better stability than SonoVue®, but without significant difference (p = 0.0711, T = -3.547, df = 2). In the 2D-CEUS conditions, the average CVs of OC-MBs group and SonoVue® group were 0.68 ±0.15 and 0.41 ±0.17 (p = 0.2747, T = 1.490, df = 2), respectively.

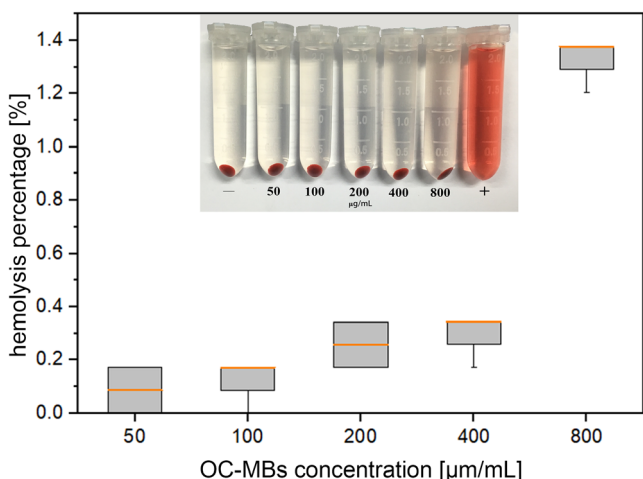


Fig. 4. Hemolysis caused by octafluoropropane-loaded cerasomal microbubbles (OC-MBs) at different concentrations. Deionized water was used as a positive control and phosphate-buffered saline (PBS) was used as a negative control. The data is shown in box and whisker plot format. The median value is displayed inside the “box” with orange line. The upper side and lower side of the “box” refer to the 1st quartile and the 3rd quartile. The maximum and minimum values are displayed with vertical lines connecting the points to the “box”

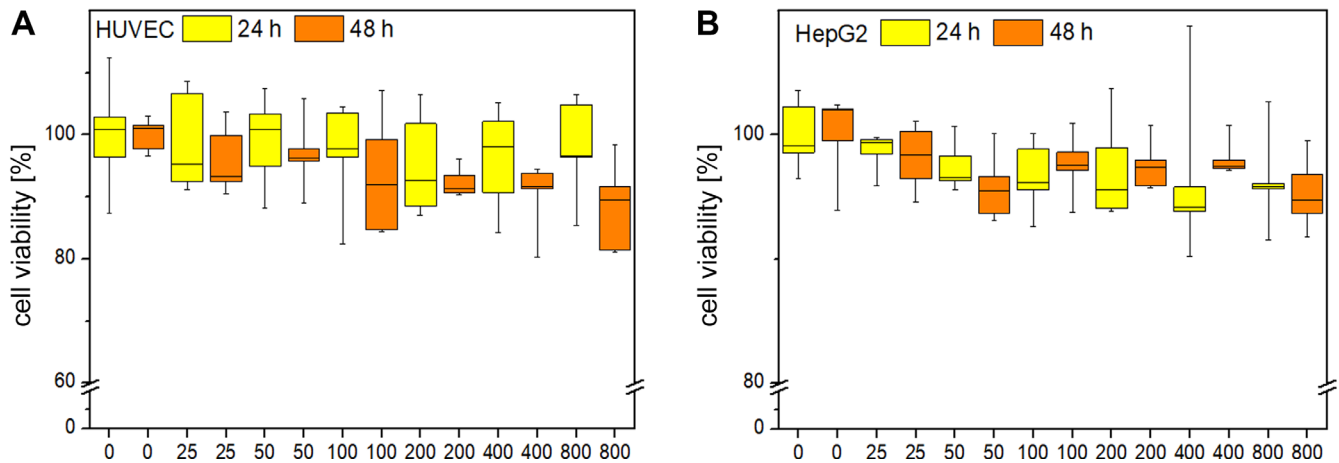


Fig. 5. In vitro cell viability of human umbilical vein endothelial cells (HUVEC) (A) and HepG2 cells (B) incubated with octafluoropropane-loaded cerasomal microbubbles (OC-MBs) at different concentrations for 24 h and 48 h. The data is shown in box and whisker plot format. The median value is displayed inside the “box” with brown line. The upper side and lower side of the “box” refer to the 1st quartile and the 3rd quartile. The maximum and minimum values are displayed with vertical lines connecting the points to the “box”. The yellow “box” refers to the results of 24 h, while the orange “box” refers to the results of 48 h

Table 1. The peak intensity (PI) values and coefficient of variation (CV) of 2 ultrasound contrast agents (UCA) in different perfusion models using 3D-CEUS

Length of perfusion model [cm]	UCA	PI (AU×10 ⁻⁶)			CV
		0°	45°	90°	
8	OC-MBs	1.35 ±0.19	1.05 ±0.00	0.73 ±0.01	29.72%
	SonoVue®	0.20 ±0.13	0.19 ±0.00	0.42 ±0.00	49.16%
16	OC-MBs	3.36 ±0.13	4.51 ±0.16	4.08 ±0.11	14.58%
	SonoVue®	3.55 ±0.09	1.61 ±0.05	2.13 ±0.07	41.40%
32	OC-MBs	2.66 ±0.05	7.48 ±0.10	4.16 ±0.10	51.77%
	SonoVue®	1.67 ±0.12	0.84 ±0.01	3.07 ±0.00	60.71%

CEUS – contrast-enhanced ultrasound; OC-MBs – octafluoropropane-loaded cerasomal microbubbles.

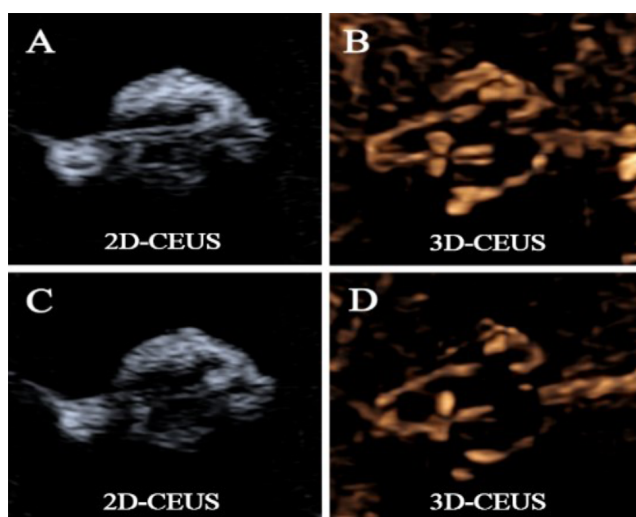


Fig. 6. Two-dimensional contrast-enhanced ultrasound (2D-CEUS) and three-dimensional contrast-enhanced ultrasound (3D-CEUS) images of 32 cm perfusion model: A,B. Octafluoropropane-loaded cerasomal microbubbles (OC-MBs); C,D: SonoVue®

Correlation between the actual perfusion volume and the weighted PI

In our study, the weighted PI was defined as the average PIs of 3 different planes (0°, 45° and 90°) in the same conditions. For 2D-CEUS, the weighted PIs of OC-MBs group of these 3 perfusion models were 0.92, 6.37 and 6.57, respectively, while the corresponding values of SonoVue® group were 0.57, 3.52 and 2.11, respectively. For 3D-CEUS, the weighted PIs of OC-MBs group were 0.96, 3.99 and 4.77, respectively. By contrast, the corresponding values of SonoVue® group were 0.27, 2.43 and 1.86, respectively (Table 4).

As the weighted PIs presented the normal distribution, the correlation between the weighted PI and the perfusion volume (1:2:4) of the in vitro model was evaluated with Pearson’s correlation analysis. As for 3D-CEUS conditions, the r-value of the weighted PI and perfusion ratio using OC-MBs group and SonoVue® were 0.8685 ($p = 0.3302$) and 0.5643 ($p = 0.6183$), respectively, while that of 2D-CEUS conditions were 0.7760 ($p = 0.4345$) and 0.3513 ($p = 0.7715$), respectively (Table 4). The OC-MBs group had higher correlation between the perfusion volume and quantitative CEUS value compared to the SonoVue® group

Table 2. The peak intensity (PI) values and coefficient of variation (CV) of 2 ultrasound contrast agents (UCA) in different perfusion model using 2D-CEUS

Length of perfusion model [cm]	UCA	PI (AU×10 ⁻⁴)			CV
		0°	45°	90°	
8	OC-MBs	1.55 ±0.00	1.00 ±0.01	0.20 ±0.00	73.75%
	SonoVue®	0.42 ±0.00	1.05 ±0.01	0.23 ±0.01	75.60%
16	OC-MBs	9.94 ±0.00	3.45 ±0.00	5.71 ±0.01	51.71%
	SonoVue®	3.12 ±0.00	2.77 ±0.00	4.68 ±0.11	28.94%
32	OC-MBs	2.89 ±0.00	12.66 ±0.00	4.17 ±0.16	80.78%
	SonoVue®	2.57 ±0.00	1.80 ±0.00	1.96 ±0.11	19.24%

CEUS – contrast-enhanced ultrasound; OC-MBs – octafluoropropane-loaded cerasomal microbubbles.

Table 3. Paired sample t-test was used to compare the mean CVs of 3D-CEUS and 2D-CEUS and mean CVs of OC-MBs group and SonoVue® group in the 3D-CEUS group and 2D-CEUS group

Values	CV of 3D-CEUS	CV of 2D-CEUS	3D-CEUS group		2D-CEUS group	
			CV of OC-MBs group	CV of SonoVue® group	CV of OC-MBs group	CV of SonoVue® group
Mean ±SD	0.41 ±0.17	0.55 ±0.26	0.32 ±0.19	0.50 ±0.10	0.68 ±0.15	0.41 ±0.17
T	-1.009		-3.547		1.490	
df	5		2		2	
p-value	0.3592		0.0711		0.2747	

CV – coefficient of variation; 2D-CEUS – two-dimensional contrast-enhanced ultrasound; 3D-CEUS – three-dimensional contrast-enhanced ultrasound; OC-MBs – octafluoropropane-loaded cerasomal microbubbles; SD – standard deviation; df – degrees of freedom.

Table 4. The weighted peak intensity (PI) (the average value of PI at 0°, 45° and 90° planes) values of different ultrasound contrast agents, perfusion models and contrast-enhanced ultrasound mode, and the correlation between weighted PIs and the perfusion volume. Pearson's correlation analysis was used to determine the correlation between weighted PI and perfusion volume (1:2:4)

Perfusion ratio	2D-CEUS (n = 3)		3D-CEUS (n = 3)	
	OC-MBs	SonoVue®	OC-MBs	SonoVue®
	weighted PI (AU×10 ⁻⁴)	weighted PI (AU×10 ⁻⁶)	weighted PI (AU×10 ⁻⁴)	weighted PI (AU×10 ⁻⁶)
1	0.92	0.57	0.96	0.27
2	6.37	3.52	3.99	2.43
4	6.57	2.11	4.77	1.86
r-value*	0.7760	0.3513	0.8685	0.5643
p-value	0.4345	0.7715	0.3302	0.6183

* r-value – correlation coefficient between weighted PI and perfusion volume (1:2:4); 2D-CEUS – two-dimensional contrast-enhanced ultrasound; 3D-CEUS – three-dimensional contrast-enhanced ultrasound; OC-MBs – octafluoropropane-loaded cerasomal microbubbles.

in 2D- and 3D-CEUS. The OC-MBs were technically feasible and they may have the potential to improve the accuracy of tumor perfusion assessment.

Discussion

The spatial distribution of blood vessels is closely related to the nature of the tumor. However, due to the necrosis, bleeding and hypoxia of the tumor, there is a large

heterogeneity within the tumor, which causes large intra-volume heterogeneities in quantitative perfusion parameters.²⁴ Two previous animal studies have shown that a small deviation in transducer position could result in quantitative errors up to 40.3%²⁵ and plane to plane variation of parametric perfusion maps could be up to 22%.²⁶ In order to solve this problem, real-time 3D-CEUS and monodisperse microbubbles were used to explore whether the measurement variation could be reduced and whether it could improve the correlation between quantitative analysis and actual blood flow.

With the help of contrast agent, the traditional 2D-CEUS greatly improves the ability of detecting tumor microvessels. However, 2D-CEUS only shows tumor blood vessels through a single plane and it cannot fully show its vascular characteristics if the blood vessels are rich or poorly positioned. The 3D-CEUS was developed to solve this problem. The 3D technique can show the spatial relationship of vascular structure after post-acquisition reconstruction. Previous study has shown that real-time 3D-CEUS could overcome sampling errors in tumors by imaging the tumor as a whole.^{27,28} However, based on the testing of our setup, the average CV of 3D-CEUS was slightly lower than that of 2D-CEUS (p = 0.3592) without significant difference. The reason might be that the perfusion model was not complex enough to simulate the internal structure of the tumor.

In the OC-MBs group, as well as in the SonoVue® group, the r-values of the weighted PI and perfusion ratio were higher when 3D-CEUS was used as compared to 2D-CEUS.

As 3D-CEUS could carry on with a volumetric imaging system, multiple planes could be captured simultaneously. The continuity and spatial relationships of the blood vessels were more clearly displayed with 3D-CEUS.⁶ As a result, the quantitative measurement from a single 3D plane is more representative than results obtained in 2D.²⁴

Another important component of CEUS is UCA. As a kind of phospholipid membrane microbubbles, SonoVue[®] can generate nonlinear harmonic signals under ultrasound scanning and has good contrast effects, which has been proven through research and has been widely used in 2D-CEUS.²⁹ In our preliminary studies, we found that for quantitative analysis, 3D-CEUS had better stability, accuracy and feasibility than 2D in both, in vitro as well as in vivo models.^{7,30} However, the phospholipid membrane of SonoVue[®] can easily burst under high energy ultrasonic irradiation and uneven particle size will affect the quantitative results. Therefore, in order to optimize the accuracy of quantitative 3D-CEUS, a new kind of monodisperse UCA with better stability is needed.

Si-lipid is a new type of organic-inorganic composite lipid synthesized from organic alkoxy silanes and lipid molecules. The double-layer vesicle structure with silica framework on the surface has higher morphological stability than traditional lipid vesicles. In recent years, there have been studies focused on the application of Si-lipid in UCA production.^{31–33} As for loaded gas, perfluorocarbon gas, such as OFP,³⁴ has extremely low water solubility and good biocompatibility, which can effectively prolong the durability of microbubbles.^{35,36} Therefore, in this study, Si-lipid and OFP were chosen to prepare OC-MBs. The CaCO₃ template method was applied to maintain the uniformity of microbubble size. Our study showed that the OC-MBs microbubbles had higher homogeneity with size distribution of 2.0 μm. As a new kind of ultrasound contrast agent, the cytotoxicity and blood biocompatibility are vital to its biomedical application. The OC-MBs have negligible hemolytic activity, present prominent biocompatibility and may have the potential to be used as new UCAs in vivo.

In the present study, under the condition that the microbubble concentration was controlled at about 4×10⁶/mL, the imaging effects of both SonoVue[®] and OC-MBs group had no significant difference in 2D-CEUS; as for 3D-CEUS, the continuity, integrity and signal strength of the phantom were significantly better in OC-MBs group than those of the SonoVue[®] group (Fig. 6). After quantitative analysis, the PI of the OC-MBs has shown better stability than SonoVue[®] in 3D-CEUS condition (Table 1). It shows that under the protection of silica framework, OC-MBs have better stability and imaging capability than SonoVue[®]. The results of the Pearson's linear correlation test show that there was a linear correlation trend between the quantitative results and the actual perfusion volume, and compared with SonoVue[®], OC-MBs have a trend of optimizing quantitative CEUS.




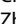
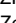
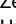




Limitations

We acknowledge several limitations of this study. First, the acoustic properties of the silicone tube used in the in vitro model are still different from the blood vessel. If better materials are to be found in the future, it is expected to reduce the impact of sound attenuation on the results. Second, only 3 in vitro models were used in this study, and more models should be involved to mimic the heterogeneity of in vivo target.

Conclusions

In the present study, we successfully prepared monodisperse OFP-loaded cerasomal microbubbles (OC-MBs) with high stability, size uniformity and biocompatibility. Our in vitro experiments showed that OC-MBs have the potential in acquiring more stable quantitative CEUS value, as compared to the SonoVue[®] in 3D-CEUS condition. The combination of 3D-CEUS and OC-MBs can reflect perfusion volume more precisely and may be a potential way to reduce quantitative heterogeneity.

ORCID iDs

Qiao Zheng  <https://orcid.org/0000-0002-3040-2137>
 Si-Min Ruan  <https://orcid.org/0000-0002-1121-3664>
 Chun-Yang Zhang  <https://orcid.org/0000-0002-4696-0176>
 Zhong Cao  <https://orcid.org/0000-0003-4004-1037>
 Ze-Rong Huang  <https://orcid.org/0000-0003-3388-8571>
 Huan-Ling Guo  <https://orcid.org/0000-0002-5806-5339>
 Xiao-Yan Xie  <https://orcid.org/0000-0002-9761-9525>
 Ming-De Lu  <https://orcid.org/0000-0002-9771-8144>
 Wei Wang  <https://orcid.org/0000-0002-9485-583X>
 Li-Da Chen  <https://orcid.org/0000-0001-9904-2195>

References

- Jung EM, Wiggermann P, Greis C, et al. First results of endocavity evaluation of the microvascularization of malignant prostate tumors using contrast enhanced ultrasound (CEUS) including perfusion analysis: First results. *Clin Hemorheol Microcirc.* 2012;52(2–4): 167–177. doi:10.3233/CH-2012-1594
- Shan QY, Chen LD, Zhou LY, et al. Focal lesions in fatty liver: If quantitative analysis facilitates the differentiation of atypical benign from malignant lesions. *Sci Rep.* 2016;6:18640. doi:10.1038/srep18640
- Kapetas P, Clauser P, Woitek R, et al. Quantitative multiparametric breast ultrasound: Application of contrast-enhanced ultrasound and elastography leads to an improved differentiation of benign and malignant lesions. *Invest Radiol.* 2019;54(5):257–264. doi:10.1097/RLI.0000000000000543
- Maxeiner A, Fischer T, Schwabe J, et al. Contrast-enhanced ultrasound (CEUS) and quantitative perfusion analysis in patients with suspicion for prostate cancer. *Ultraschall Med.* 2019;40(3):340–348. doi:10.1055/a-0594-2093
- Williams R, Hudson JM, Lloyd BA, et al. Dynamic microbubble contrast-enhanced US to measure tumor response to targeted therapy: A proposed clinical protocol with results from renal cell carcinoma patients receiving antiangiogenic therapy. *Radiology.* 2011;260(2): 581–590. doi:10.1148/radiol.11101893
- Dong FJ, Xu JF, Du D, et al. 3D analysis is superior to 2D analysis for contrast-enhanced ultrasound in revealing vascularity in focal liver lesions: A retrospective analysis of 83 cases. *Ultrasonics.* 2016;70: 221–226. doi:10.1016/j.ultras.2016.05.007

7. Ruan SM, Zheng Q, Wang Z, et al. Comparison of real-time two-dimensional and three-dimensional contrast-enhanced ultrasound to quantify flow in an in vitro model: A feasibility study. *Med Sci Monit*. 2019;25:10029–10035. doi:10.12659/msm.919160
8. Stride E, Saffari N. Microbubble ultrasound contrast agents: A review. *Proc Inst Mech Eng H*. 2003;217(6):429–447. doi:10.1243/09544110360729072
9. Kollmann C, Putzer M. Ultrasound contrast agents: Physical basics [in German]. *Radiologe*. 2005;45(6):503–512. doi:10.1007/s00117-005-1188-z
10. Frinking P, Segers T, Luan Y, Tranquart F. Three decades of ultrasound contrast agents: A review of the past, present and future improvements. *Ultrasound Med Biol*. 2020;46(4):892–908. doi:10.1016/j.ultrasmedbio.2019.12.008
11. Segers T, Kruijzinga P, Kok MP, Lajoinie G, de Jong N, Versluis M. Mono-disperse versus polydisperse ultrasound contrast agents: Non-linear response, sensitivity, and deep tissue imaging potential. *Ultrasound Med Biol*. 2018;44(7):1482–1492. doi:10.1016/j.ultrasmedbio.2018.03.019
12. Chen M, Wang WP, Jia WR, et al. Three-dimensional contrast-enhanced sonography in the assessment of breast tumor angiogenesis: Correlation with microvessel density and vascular endothelial growth factor expression. *J Ultrasound Med*. 2014;33(5):835–846. doi:10.7863/ultra.33.5.835
13. Zhang C, Wang Z, Wang C, et al. Highly uniform perfluoropropane-loaded cerasomal microbubbles as a novel ultrasound contrast agent. *ACS Appl Mater Interfaces*. 2016;8(24):15024–15032. doi:10.1021/acsami.5b03668
14. Katagiri K, Hashizume M, Ariga K, Terashima T, Kikuchi J. Preparation and characterization of a novel organic-inorganic nanohybrid “cerasome” formed with a liposomal membrane and silicate surface. *Chemistry*. 2007;13(18):5272–5281. doi:10.1002/chem.200700175
15. Zhang CY, Cao Z, Zhu WJ, Liu J, Jiang Q, Shuai XT. Highly uniform and stable cerasomal microcapsule with good biocompatibility for drug delivery. *Colloids Surf B Biointerfaces*. 2014;116:327–333. doi:10.1016/j.colsurfb.2014.01.013
16. Tong W, Dong W, Gao C, Mohwald H. Charge-controlled permeability of polyelectrolyte microcapsules. *J Phys Chem B*. 2005;109(27):13159–13165. doi:10.1021/jp0511092
17. Zhang C, Wang Z, Wang C, et al. Highly uniform perfluoropropane-loaded cerasomal microbubbles as a novel ultrasound contrast agent. *ACS Appl Mater Interfaces*. 2016;8(24):15024–15032. doi:10.1021/acsami.5b03668
18. Schellinger JG, Pahang JA, Johnson RN, et al. Melittin-grafted HPMA-oligolysine based copolymers for gene delivery. *Biomaterials*. 2013;34(9):2318–2326. doi:10.1016/j.biomaterials.2012.09.072
19. Parnham MJ, Wetzig H. Toxicity screening of liposomes. *Chem Phys Lipids*. 1993;64(1–3):263–274. doi:10.1016/0009-3084(93)90070-j
20. Saxena V, Diaz A, Clearfield A, Batteas JD, Hussain MD. Zirconium phosphate nanoplatelets: A biocompatible nanomaterial for drug delivery to cancer. *Nanoscale*. 2013;5(6):2328–2336. doi:10.1039/c3nr34242e
21. Shen M, Cai H, Wang X, et al. Facile one-pot preparation, surface functionalization, and toxicity assay of APTS-coated iron oxide nanoparticles. *Nanotechnology*. 2012;23(10):105601. doi:10.1088/0957-4484/23/10/105601
22. Fischer D, Li YX, Ahlemeyer B, Krieglstein J, Kissel T. In vitro cytotoxicity testing of polycations: Influence of polymer structure on cell viability and hemolysis. *Biomaterials*. 2003;24(7):1121–1131. doi:10.1016/s0142-9612(02)00445-3
23. Lassau N, Chami L, Benatsou B, Peronneau P, Roche A. Dynamic contrast-enhanced ultrasonography (DCE-US) with quantification of tumor perfusion: A new diagnostic tool to evaluate the early effects of antiangiogenic treatment. *Eur Radiol*. 2007;17(Suppl 6):F89–F98. doi:10.1007/s10406-007-0233-6
24. El Kaffas A, Sigrist RMS, Fisher G, et al. Quantitative three-dimensional dynamic contrast-enhanced ultrasound imaging: First-in-human pilot study in patients with liver metastases. *Theranostics*. 2017;7(15):3745–3758. doi:10.7150/thno.20329
25. Hoyt K, Sorace A, Saini R. Quantitative mapping of tumor vascularity using volumetric contrast-enhanced ultrasound. *Invest Radiol*. 2012;47(3):167–174. doi:10.1097/RLI.0b013e318234e6bc
26. Feingold S, Gessner R, Guracar IM, Dayton PA. Quantitative volumetric perfusion mapping of the microvasculature using contrast ultrasound. *Invest Radiol*. 2010;45(10):669–674. doi:10.1097/RLI.0b013e3181ef0a78
27. Wang HJ, Hristov D, Qin JL, Tian L, Willmann JK. Three-dimensional dynamic contrast-enhanced US imaging for early antiangiogenic treatment assessment in a mouse colon cancer model. *Radiology*. 2015;277(2):424–434. doi:10.1148/radiol.2015142824
28. Wang H, Kaneko OF, Tian L, Hristov D, Willmann JK. Three-dimensional ultrasound molecular imaging of angiogenesis in colon cancer using a clinical matrix array ultrasound transducer. *Invest Radiol*. 2015;50(5):322–329. doi:10.1097/RLI.0000000000000128
29. Leong-Poi H, Song J, Rim SJ, Christiansen J, Kaul S, Lindner JR. Influence of microbubble shell properties on ultrasound signal: Implications for low-power perfusion imaging. *J Am Soc Echocardiogr*. 2002;15(10 Pt 2):1269–1276. doi:10.1067/mje.2002.124516
30. Zheng Q, Zhang JC, Wang Z, et al. Assessment of angiogenesis in rabbit orthotopic liver tumors using three-dimensional dynamic contrast-enhanced ultrasound compared with two-dimensional DCE-US. *Jpn J Radiol*. 2019;37(10):701–709. doi:10.1007/s11604-019-00861-z
31. Katagiri K, Hamasaki R, Ariga K, Kikuchi J. Layered paving of vesicular nanoparticles formed with cerasome as a bioinspired organic-inorganic hybrid. *J Am Chem Soc*. 2002;124(27):7892–7893. doi:10.1021/ja0259281
32. Liang XL, Gao J, Jiang LD, et al. Nanohybrid liposomal cerasomes with good physiological stability and rapid temperature responsiveness for high intensity focused ultrasound triggered local chemotherapy of cancer. *ACS Nano*. 2015;9(2):1280–1293. doi:10.1021/nn507482w
33. Steinberg Y, Schroeder A, Talmon Y, et al. Triggered release of aqueous content from liposome-derived sol-gel nanocapsules. *Langmuir*. 2007;23(24):12024–12031. doi:10.1021/la702311f
34. Koch M, Franck CM. Partial discharges and breakdown in C3F8. *J Phys D Appl Phys*. 2014;47(40):11. doi:10.1088/0022-3727/47/40/405203
35. Kabalnov A, Bradley J, Flaim S, et al. Dissolution of multicomponent microbubbles in the bloodstream: 2. Experiment. *Ultrasound Med Biol*. 1998;24(5):751–760. doi:10.1016/s0301-5629(98)00033-7
36. Kabalnov A, Klein D, Pelura T, Schutt E, Weers J. Dissolution of multicomponent microbubbles in the bloodstream: 1. Theory. *Ultrasound Med Biol*. 1998;24(5):739–749. doi:10.1016/s0301-5629(98)00034-9